Supplementary information

Influence of Solution- and Thermal Annealing-Process on Sub-Nanometer-Ordered Organic–Organic Interface Structure of Organic Light-Emitting Devices

Satoru Ohisa,[a] Yong-Jin Pu,[a]* Norifumi L. Yamada,[b] Go Matsuba,[a] and Junji Kido[a]*

[a]Department of Organic Materials Science, Graduate School of Organic Materials Science, Yamagata University, Yonezawa, Yamagata, 992-8510 Japan.

[b]Institute of Material Structure Science, High-Energy Accelerator Research Organization (KEK), 203-1 Shirakata, Tokai, Naka 319-1106, Japan

E-mail: pu@yz.yamagata-u.ac.jp; kid@yz.yamagata-u.ac.jp

Experimental details

Materials. Chemical structures of the materials used in this work are shown in **Figure S1**. Materials were purchased from commercial sources, except for BCzBP and BCzBP-d[14], which were synthesized according to established procedures.[1, 2] The deuteration ratio of the carbazole moiety was approximately 94%, as determined by ^{1}H-NMR analysis. BCzBP, BCzBP-d[14], Ir(mppy)[3], and TPBi were purified by sublimation. Other materials were used as received. PTPD (catalog No. ADS254BE) was purchased from American Dye Source, Inc. Weight-average and number-average molecular weights, as determined by gel permeation chromatography using polystyrene standards, were 78,000 and 28,000, respectively. Ir(mppy)[3], TPBi, and Liq were purchased from e-Ray Optoelectronics Technology Co., Ltd. PEDOT:PSS (*Clevios*™ P VP CH 8000) was purchased from Heraeus Materials Technology.
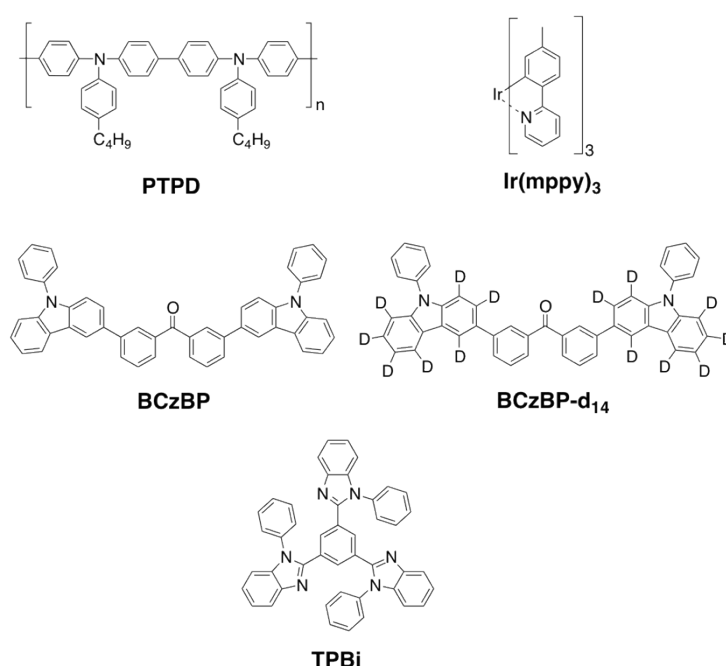
Figure S1. Chemical structures of the compounds used in this work.

Film preparation. The substrates were rinsed with acetone and 2-propanol and then dried under a stream of clean nitrogen. Prior to film formation, the substrates were cleaned with a

UV–ozone cleaner for 20 min. Films were formed by spin coating or by evaporation under high vacuum (<5.0 × 10^{-5} Pa). PTPD and BCzBP (or BCzBP-d$_{14}$):Ir(mppy)$_3$ (91:9 weight ratio) films were spin coated under the same conditions used in our previous work.[2] TPBi was formed from an alcohol solution. PTPD and BCzBP (or BCzBP-d$_{14}$):Ir(mppy)$_3$ films were annealed at 135°C and 115°C for 10 min in a N$_2$-purged insulating container, respectively. The TPBi film was annealed at 100°C for 5 min, followed by 115°C for 10 min in the N$_2$-purged insulating container. PEDOT:PSS dispersion liquid was spin coated and annealed at 200°C for 10 min in air. Thicknesses of the resulting films were determined using NR results or a surface profilometer (Veeco Dektak8).

Neutron reflectometry (NR). Pre-cleaned cut Si wafers (KST World Corp., Japan) of 45 mm × 45 mm area were used without removal of the native oxide layer. Films were formed by spin coating or evaporation onto the Si wafers. Neutron reflectivity was recorded using the single-frame mode of the soft interface analyzer (SOFIA) horizontal-type time-of-flight neutron reflectometer (2.0 Å < λ < 8.8 Å) at J-PARC (Japan Proton Accelerator Research Complex)/MLF (Materials and Life Science Experimental Facility).[3, 4] Neutron pulses were recorded using a two-dimensional scintillation counter, which consisted of an AR3239 photomultiplier tube (Hamamatsu Photonics K. K., Hamamatsu, Japan) with a ZnS/^{6}LiF scintillator (Ohyo Koken, Fussa, Japan). Reflected beam spectra were collected at 0.30°, 0.75°, and 1.80°. Individual data points were combined. Direct beam measurements were collected under the same collimation conditions as the beam spectra collected at 0.30°, and the same time-of-flight profile used for the other angles was used. Least-squares analyses of the reflectivity profiles were performed using the Motofit reflectometry analysis program; interfacial roughness was included via a Nevot–Croce factor.[5, 6]

Fluorescence resonance energy transfer

(FRET). Pre-cleaned quartz substrates were used. A stacked film with a structure of [quartz/BCzBP:9 wt% Ir(mppy)$_3$ (40 nm)/TPBi (30 nm)] was fabricated. Each layer was sequentially formed by evaporation or spin coating. The formed films were encapsulated in glass caps with UV-cured resins and oxygen getters. Photoluminescence spectra were obtained using a HORIBA JOBIN YVON Fluoromax-4. Illuminated areas of excitation light were defined using a mask. The influence of guided light was possibly decreased by pasting black tape on the samples.

OLED fabrication and measurements. OLEDs were fabricated on pre-cleaned ITO substrates (Asahi Glass Co., Ltd.). OLEDs with the structure of [ITO (130 nm)/PEDOT:PSS (40 nm)/PTPD (20 nm)/BCzBP:9 wt% Ir(mppy)$_3$ (40 nm)/TPBi (30 nm)/Liq (1.5 nm)/Al (100 nm)] were fabricated. Here, PEDOT:PSS and PTPD were spin coated. BCzBP:9 wt% Ir(mppy)$_3$ was spin coated onto PTPD as the sEML and annealed at 115°C for 10 min. TPBi was spin coated as sTPBi onto the sEML, annealed at 100°C for 5 min, and then annealed at 115°C for 5 min. TPBi was also evaporated onto the sEML. eTPBi was either not annealed or annealed at 125°C for 10 min. Liq and Al were evaporated successively. The fabricated devices were encapsulated in glass caps with UV-cured resins and oxygen getters. All of the emission areas were 2 mm × 2 mm. The current density–voltage characteristics and luminance–voltage characteristics of the OLEDs were measured using a Keithley 2400 current source and a Konica Minolta CS-200 luminance meter, respectively. EL spectra were collected using a Konica Minolta CS-2000 spectral radiance meter. Quantum efficiencies were calculated using the Lambertian assumption.

Thermal and photophysical properties

Thermal properties were characterized using differential scanning calorimetry (Perkin Elmer Diamond DSC). The scan speed was 10°C/min. UV absorption measurements were performed using a UV–Vis–NIR spectrometer (SHIMADZU UV-3150). Optical band gaps were determined from the UV spectra. Photoluminescence spectra excited by 320-nm light were obtained using a spectrofluorometer (HORIBA JOBIN YVON Fluoromax-4). Phosphorescence spectra were obtained at 5 K under excitation by a nitrogen laser ($\lambda = 337$ nm, 50 Hz, 800-ps pulses) combined with a Hamamatsu C4334 streak scope and a Hamamatsu C4792-02 synchronous delay generator. Ionization potentials (*IP*) were determined by atmospheric UV photoelectron yield spectroscopy. Electron affinity (*EA*) values values were determined by subtracting optical band gaps from ionization potentials.

Table S1. Material characteristics.

Materials	T_g (°C)[a]	IP (eV)[b]	EA (eV)[c]	E_g (eV)[d]	T_1 (eV)[e]
PTPD	224	5.3	2.4	2.9	2.3
BCzBP	119	5.9	2.6	3.3	2.7
BCzBP-d_{14}	120	n.d.	n.d.	n.d.	n.d.
Ir(mppy)$_3$	n.d.	5.5	3.1	2.4	2.4
TPBi	122	6.2	2.7	3.5	2.7

[a]Glass-transition temperatures determined from differential scanning calorimetry measurements. [b]Ionization potentials determined from photoelectron yield spectroscopy measurements. [c]Electron affinities determined from subtraction energy gaps from the ionization potentials. [d]Energy gaps determined from UV–vis absorption measurements. [e]Lowest triplet energies determined from phosphorescence spectra.

Solvent resistances of films

PTPD, BCzBP, and Ir(mppy)$_3$ films were prepared on quartz substrates. These films were rinsed with corresponding upperlayer coating solvents. UV–vis absorption spectra of these films were collected before and after the rinsing (**Figure S2**).
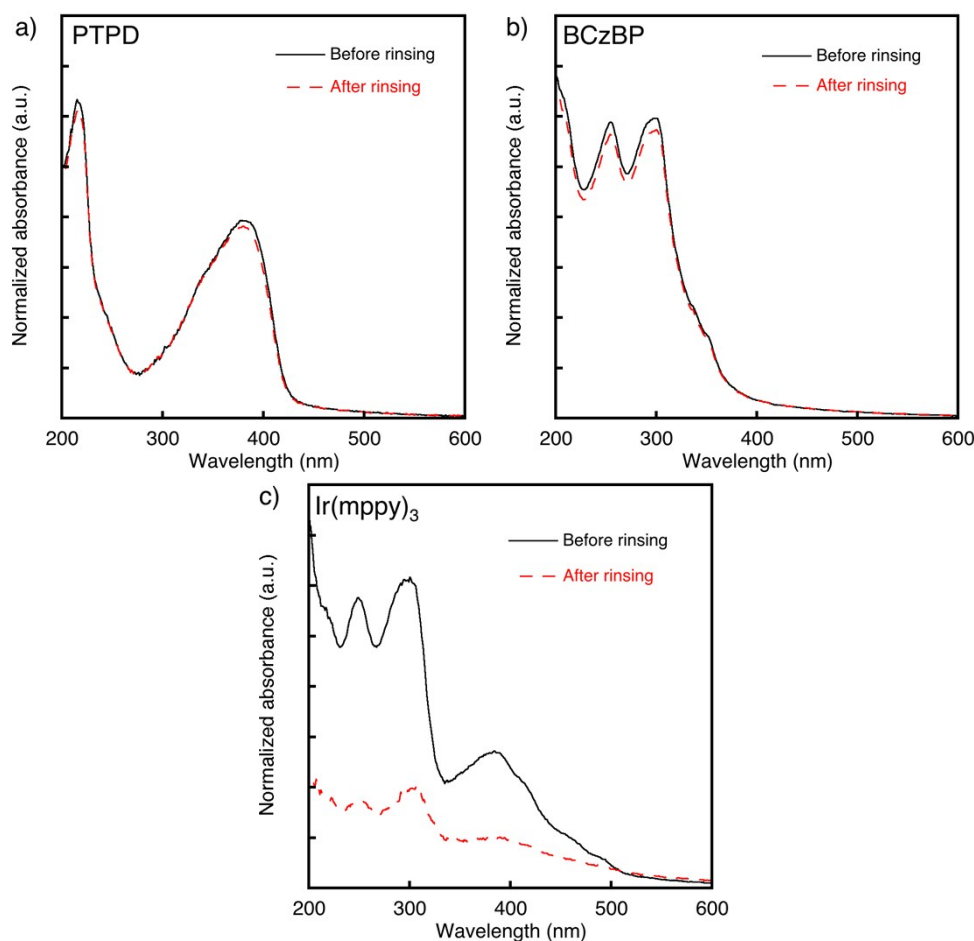
Figure S2. Normalized UV absorption spectra before and after rinsing of single-layer films: a) PTPD, b) BCzBP, and c) Ir(mppy)$_3$.

Evaluation of single-layer films by NR

Stacked films were analyzed on the basis of the results from analyses of single-layer films. Therefore, we analyzed single-layer films by NR. We have already reported the analyses of PTPD and BCzBP-d$_{14}$:9 wt% Ir(mppy)$_3$ single-layer films in our previous work.[2] PTPD, BCzBP-d$_{14}$:9 wt% Ir(mppy)$_3$, and TPBi were spin coated onto a Si wafer. Each film was annealed at 135°C for 10 min; 115°C for 10 min; or 100°C for 5 min followed by 115°C for 10 min. These temperatures are higher than the boiling points of each solvent used to form the films. Furthermore, these annealing temperatures are lower than the T_gs of the compounds (i.e., 224°C for PTPD, 120°C for BCzBP-d$_{14}$, and 124°C for TPBi). BCzBP-d$_{14}$:9 wt% Ir(mppy)$_3$ and TPBi were also evaporated onto a Si wafer under high vacuum. NR measurements of the single-layer films were

performed (**Figure S3**); the results obtained from the least-squares fits are summarized in **Table S2**. Each reflectivity curve was well fitted with a one-organic-layer model. The SLDs of sEML and eEML are high because of the use of the deuterated compound, BCzBP-d_{14}.
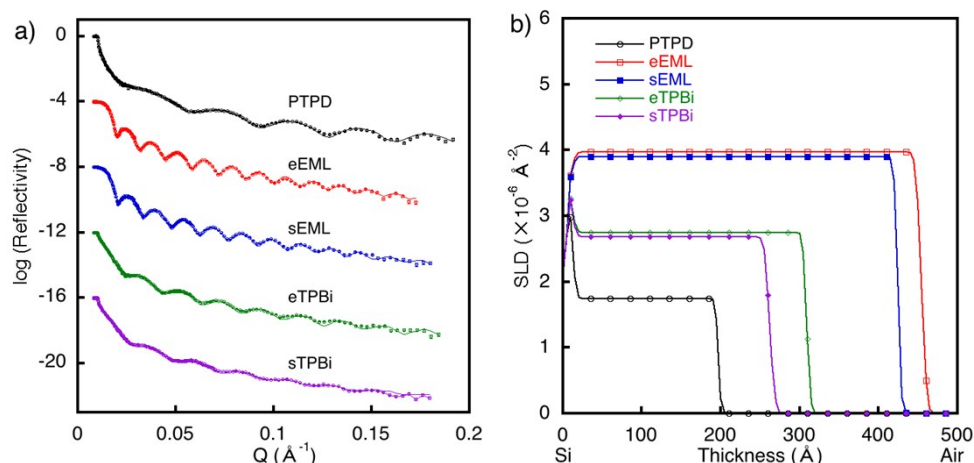

Figure S3. Neutron reflectometry results for single-layer films. a) Reflectivity profiles and b) SLD profiles of Si/PTPD (open circles), Si/eEML (open squares), Si/sEML (closed squares), Si/eTPBi (open diamonds), and Si/sTPBi (closed diamonds). The reflectivity scale corresponds to the profile for Si/PTPD. For clarity, the other plots are successively offset by 4 log units. eEML: evaporated BCzBP-d_{14}:9 wt% Ir(mppy)$_3$; sEML: spin-coated BCzBP-d_{14}:9 wt% Ir(mppy)$_3$; eTPBi: evaporated TPBi; sTPBi: spin-coated TPBi.

Table S2. Fitting results of NR measurements.

Sample layout	PTPD	BCzBP-d_{14}:Ir(mppy)$_3$	TPBi
	d / SLD / σ [a] (Å / ×10^{-6} Å^{-2} / Å)	d / SLD / σ [a] (Å / ×10^{-6} Å^{-2} / Å)	d / SLD / σ [a] (Å / ×10^{-6} Å^{-2} / Å)
PTPD	185 / 1.74 / 4	– / – / –	– / – / –
eEML	– / – / –	442 / 3.97 / 7	– / – / –
sEML	– / – / –	413 / 3.90 / 5	– / – / –
eTPBi	– / – / –	– / – / –	297 / 2.75 / 5
sTPBi	– / – / –	– / – / –	250 / 2.68 / 7
sEML/sTPBi	– / – / –	336 / 3.64 / 60	290 / 2.96 / 5
sEML/eTPBi (w/o annealing)	– / – / –	401 / 3.87 / 5	297 / 2.72 / 5
sEML/eTPBi (115°C)	– / – / –	405 / 3.84 / 5	299 / 2.74 / 5
sEML/eTPBi (120°C)	– / – / –	414 / 3.77 / 16	288 / 2.77 / 5
sEML/eTPBi (130°C)	– / – / –	535 / 3.38 / 60	172 / 3.30 / 5
PTPD/eEML/eTPBi	185 / 1.74 / 5	433 / 3.94 / 5	298 / 2.74 / 6
PTPD/sEML/eTPBi	223 / 2.38 / 15	357 / 3.87 / 5	298 / 2.74 / 6
PTPD/sEML/sTPBi	227 / 2.40 / 14	294 / 3.64 / 60	271 / 2.96 / 5

[a]d, SLD, and σ represent thickness, scattering length density, and interfacial roughness, respectively.
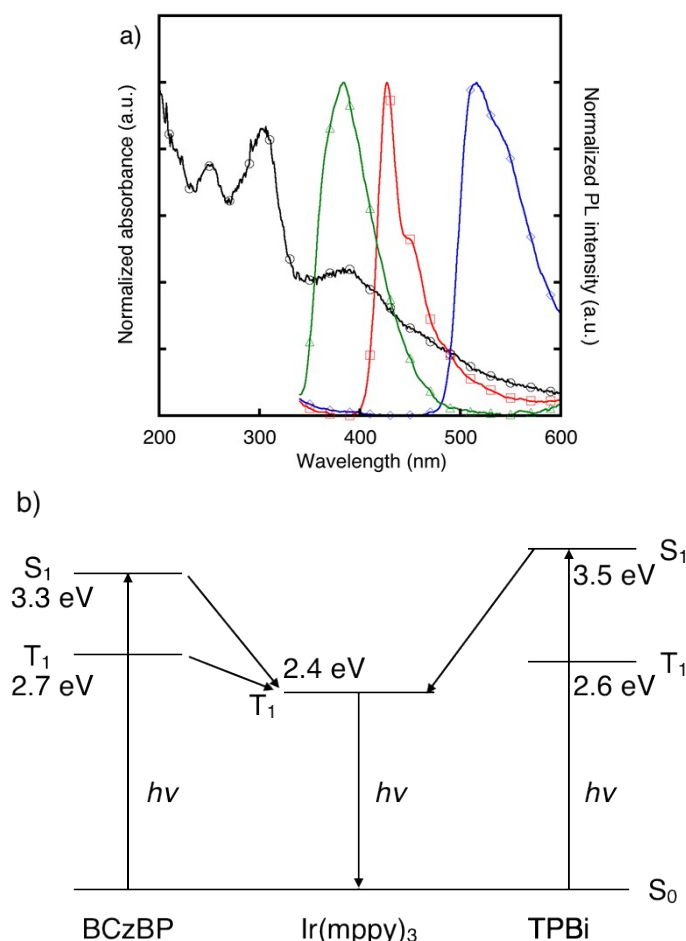
Figure S4. Normalized UV and photoluminescence spectra and a schematic of the energy transfer mechanism. a) UV absorption spectrum of Ir(mppy)$_3$ (circles) and PL spectra of BCzBP:9 wt% Ir(mppy)$_3$ (diamonds), TPBi (triangles) and PTPD (squares). b) Energy transfer mechanism.

Volume ratio estimation of each material in mixed layers

The volume ratios of each material were calculated using the SLD values of the mixed-layer and single-layer films. For example, we considered mixed layers to be constituted of two materials: A and B. The SLD values of the mixed layer and the single layers of materials A and B are represented as SLD$_{mix}$, SLD$_A$, and SLD$_B$, respectively. SLD$_{mix}$ was approximated as a linear combination of the SLD values of the corresponding single-layer films, SLD$_A$ and SLD$_B$, as follows:

$$SLD_{mix} = \varphi_A \times SLD_A + \varphi_B \times SLD_B$$

where φ_A and φ_B are the volume ratios of materials A and B in the mixed layer. We did not consider the effects of differences in the molecular packing state on the film density between the mixed-layer and the single-layer films. We also treated two kinds of materials, BCzBP-d_{14} and Ir(mppy)$_3$, as a single material that could not be separated.
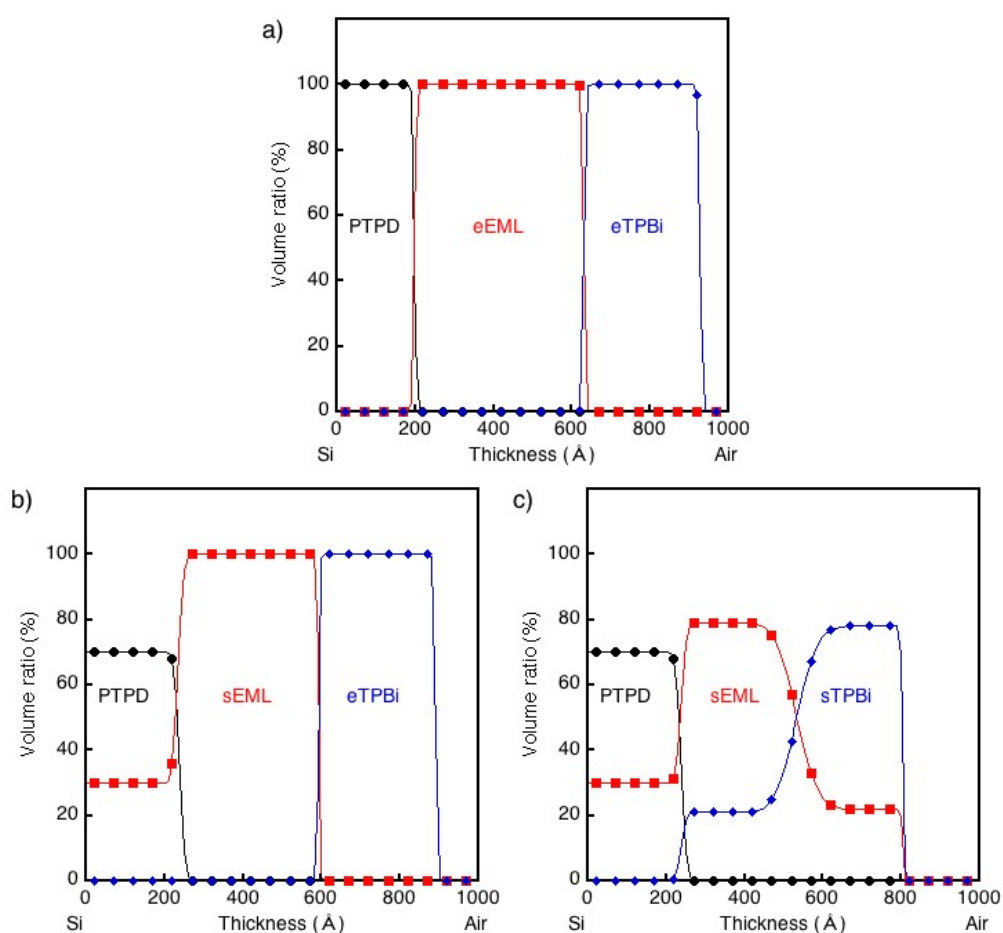
Figure S5. Materials distribution profiles of trilayer films: a) PTPD/eEML/eTPBi, b) PTPD/sEML/eTPBi, and c) PTPD/sEML/sTPBi.
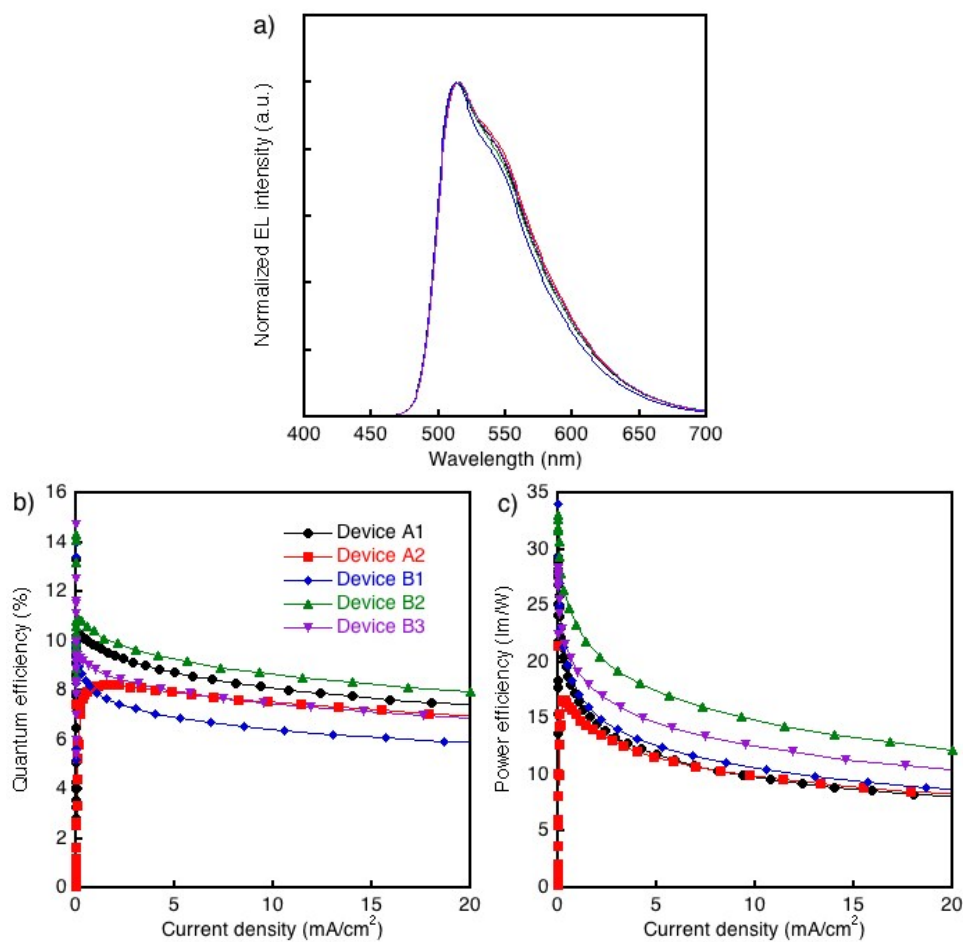
Figure S6. EL characteristics. a) EL spectra and b) quantum efficiency–current density and c) power efficiency–current density characteristics of OLEDs with sEML/sTPBi (Device A1: black closed circles), eEML (annealed)/eTPBi (annealed) (Device A2: red closed squares), eEML/eTPBi (Device B1: blue closed diamonds), sEML/eTPBi (Device B2: green triangles), and eEML (annealed)/eTPBi (Device B3: purple inverted triangles).

References

1. C.-H. Jun, Y.-J. Pu, M. Igarashi, T. Chiba, H. Sasabe, J. Kido, *Chem. Lett.* 2014, **43**, 1935-1936.
2. S. Ohisa, Y. J. Pu, N. L. Yamada, G. Matsuba, J. Kido, *ACS Appl. Mater. Interfaces* 2015, **7**, 20779-20785.
3. K. Mitamura, N. L. Yamada, H. Sagehashi, N. Torikai, H. Arita, M. Terada, M. Kobayashi, S. Sato, H. Seto, S. Goko, M. Furusaka, T. Oda, M. Hino, H. Jinnai, A. Takahara, *Polym. J.* 2012, **45**, 100-108.
4. N. L. Yamada, N. Torikai, K. Mitamura, H. Sagehashi, S. Sato, H. Seto, T. Sugita, S. Goko, M. Furusaka, T. Oda, M. Hino, T. Fujiwara, H. Takahashi, A. Takahara, *Eur. Phys. J. Plus* 2011, **126**, 108
5. A. Nelson, *J. Appl. Crystallogr.* 2006, **39**, 273-276.
6. A. Nelson, *J. Phys.: Conf. Ser.* 2010, **251**, 012094.